J. Math. Biology 12, 1 – 11 (1981)

Journal of
Mathematical
Biology

Hopf Bifurcation in a Stomatal Oscillator

R. H. Rand, S. K. Upadhyaya, J. R. Cooke, and D. W. Storti

Departments of Theoretical and Applied Mechanics and Agricultural Engineering, Cornell University, Ithaca, NY 14853, USA

Abstract. Stomata are microscopic openings in leaves of green plants which permit gas exchange. This paper presents a parameter study of a model of a stomatal oscillator first derived by Delwiche and Cooke in 1977. We prove the existence of an unstable limit cycle by using the theory of the Hopf bifurcation. Other bifurcations exhibited by the model are also discussed.

Key words: Bifurcation – Stomata – Oscillation – Nonlinear dynamics

Introduction

Green plants convert the energy of sunlight into the storable chemical energy of sugars and starches through the process of photosynthesis. Photosynthesis requires CO_2 which is available in the ambient atmosphere. Stomata are microscopic openings in the leaf surface which permit CO_2 to diffuse inward. Water vapor, however, may also diffuse through the stomatal pore, generally in an outward direction. Evaporation of water vapor is generally considered undesirable, especially in times of drought. Stomata therefore have the dual task of permitting sufficient entry of CO_2 while avoiding excessive water loss.

The stomatal pore lies between two specialized guard cells, Fig. 1. The guard cells are themselves surrounded by subsidiary cells. The pore width has been shown

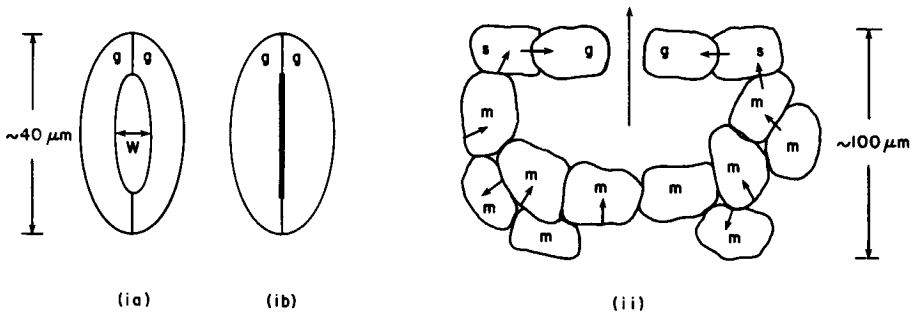

Fig. 1. The stomatal apparatus: (i) view looking onto the leaf surface, (a) pore open, (b) pore closed; (ii) cross-sectional view with arrows representing various water fluxes (see text); *g, guard cell*; *s, subsidiary cell*; *m, mesophyll cell*

0303 – 6812/81/0012/0001/$02.20

[1] to be a piecewise-linear function of the pressures in the guard and subsidiary cells:

$$w = k(c_2x - c_3y)H(c_2x - c_3y) \tag{1}$$

where w = pore width, x = hydrostatic (turgor) pressure in guard cell, y = hydrostatic (turgor) pressure in subsidiary cell, H = Heaviside step function, k, c_2, c_3 = positive constants.

In normal functioning, the stomatal pore is usually found to be open in the daytime and closed at night (thereby reducing water loss in the absence of sunlight for photosynthesis). Moreover, stomatal pores have been observed to oscillate with periods ranging from 2 to 50 minutes, even under constant environmental conditions [2]. Since the pore width w varies with time, the pressures x, y in the guard and subsidiary cells must also, from (1), be time dependent.

A model of stomatal dynamics was presented by Delwiche and Cooke [3]. The model consisted of a flow on the x, y phase plane, defined by the following differential equations:

$$\begin{aligned} \dot{x} &= -a_1x + a_2y + b_1, \\ \dot{y} &= a_3x - a_4y + b_2 + f(x,y), \\ f(x,y) &= \frac{-c_1}{1 + \dfrac{1}{c_2x - c_3y}} H(c_2x - c_3y) \end{aligned} \tag{2}$$

where again H is the Heaviside step function and where the constants a_1, a_2, a_3, a_4, b_1, b_2, c_1, c_2, c_3 are positive. We refer the reader to [3] for the derivation of these equations governing the stomatal oscillator, but note that they are based on conservation of mass for liquid and gaseous fluxes between guard cells, subsidiary cells and the rest of the plant.

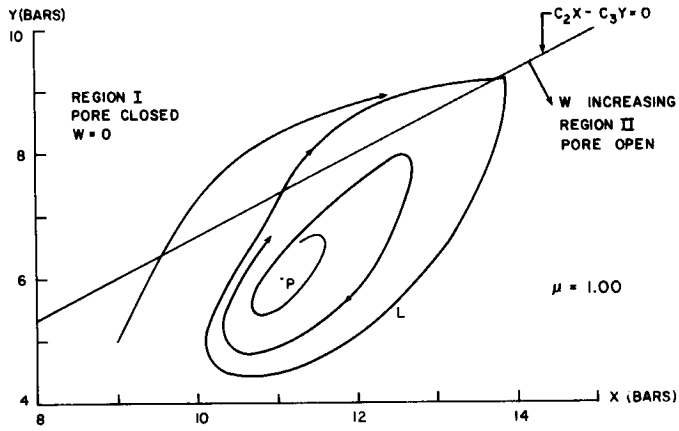

Fig. 2. Phase portrait for system (2) with $\mu = 1$ (the case considered by Delwiche and Cooke [3]). P is an unstable equilibrium point and L is a stable limit cycle

Note that the system (2) is linear above the line $c_2x = c_3y$ (region I) but is nonlinear below that line (region II), Fig. 2. From (1), this line corresponds to first closure of the stomatal pore, $w = 0$. Points in the x, y plane in region I correspond to complete closure of the pore. Points in region II correspond to an open pore, the width of the opening w being proportional to the distance from the line $c_2x = c_3y$. Note also that the vector field (2) is continuous everywhere in the xy plane, and in particular across the line $c_2x = c_3y$ since $f(x, y) = 0$ on that line.

Delwiche and Cooke (ref. [3], p. 133) chose the parameters given in Table I for their model. The resulting phase portrait (obtained by numerical integration) is shown in Fig. 2. It includes a stable limit cycle L and an unstable equilibrium point P. The limit cycle corresponds to an autonomous oscillation which may be described in words as follows: Water evaporating from the wet mesophyll and subsidiary cell walls diffuses through the stomatal pore to the leaf exterior. This water is replaced both by a flux brought to the leaf mesophyll and subsidiary cell walls from the roots via the vascular system, as well as by water diffusing passively from the guard cells to the subsidiary cells. The resulting decrease in hydrostatic pressure in the guard cells causes the stomatal pore width to decrease. A smaller pore width slows the rate of evaporation and causes water to accumulate in the mesophyll and subsidiary cells. In response to this accumulation, water diffuses back to the guard cells, increasing their hydrostatic pressure and increasing the pore width. See Fig. 1.

In this work we shall embed Delwiche and Cooke's choice of parameter values in a one-parameter family of systems (2) with parameter μ. Their system (Fig. 2) corresponds to $\mu = 1$. Physically an increase in μ corresponds to an increase in the osmotic contents of the guard cell ($\bar{\pi}_g$ in the notation of [3]).

The purpose of this work is to investigate the qualitative behavior of this family of dynamical systems as μ is tuned in the neighborhood of unity. We shall show that for μ between 0.8 and 1.2 the phase portrait may differ considerably from that of Fig. 2. In particular for a range of values of μ larger than $\mu_0 = 1.01026$ the

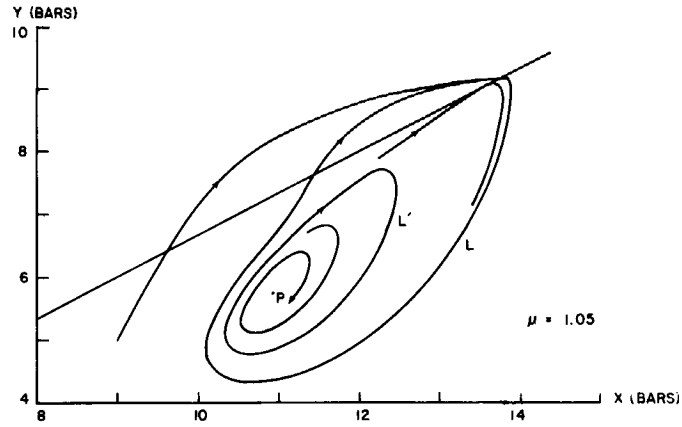

Fig. 3. Phase portrait for system (2) with $\mu = 1.05$. P is stable equilibrium point, L is a stable limit cycle and L' is an unstable limit cycle

equilibrium point P becomes stable, an unstable limit cycle (denoted by L' in Fig. 3) exists, and the stable limit cycle L persists.

The process by which the limit cycle L' is created as the equilibrium point P goes from unstable to stable with a change in the parameter μ is called a Hopf bifurcation. We shall prove the existence of an unstable limit cycle L' for system (2) by appealing to the theory of Hopf bifurcations [4].

We shall also investigate the bifurcations which determine the fate of the limit cycles L, L' for values of μ sufficiently far from μ_0.

We will conclude with a discussion of the biological significance of these dynamical considerations.

Theory of the Hopf Bifurcation

This discussion is based on the 1976 work of Marsden and McCracken [4]. Consider the general system

$$\dot{\xi} = F(\xi, \eta, \mu),$$
$$\dot{\eta} = G(\xi, \eta, \mu) \tag{3}$$

where $F(\xi, \eta, \mu)$ and $G(\xi, \eta, \mu)$ are C^k $(k \geqslant 4)$. We assume that the origin $\xi = 0$, $\eta = 0$ is an equilibrium position of this system for all μ.

Now consider the stability of the equilibrium position (0, 0). We assume that as μ increases through μ_0 the origin changes from an unstable focus to a stable focus. That is, the eigenvalues λ of the linearized system corresponding to (3) are of the form

$$\lambda = r(\mu) \pm i\omega(\mu)$$

where the real part r is positive for $\mu < \mu_0$ and is negative for $\mu > \mu_0$, and where $\omega(\mu_0) \neq 0$. We also assume (for technical reasons) that $dr/d\mu \neq 0$ at $\mu = \mu_0$.

In such a case, we are guaranteed that (3) possesses a periodic motion for μ near μ_0. There are two generic possibilities:

Either i) a limit cycle exists only for $\mu > \mu_0$, in which case it is unstable, or

ii) a limit cycle exists only for $\mu < \mu_0$, in which case it is stable. See Fig. 4.

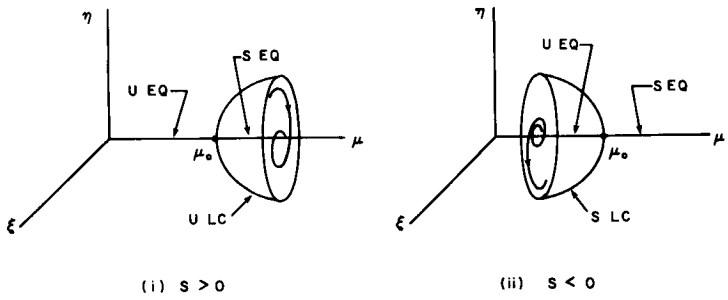

Fig. 4. Two kinds of Hopf bifurcations: (i) bifurcation of an unstable limit cycle, (ii) bifurcation of a stable limit cycle; *U, unstable*; *S, stable*; *EQ equilibrium*; *LC, limit cycle*

Marsden and McCracken give the following test for the stability of the limit cycle (see section 4A in ref. [4]). Firstly we assume that the coordinates ξ, η have been chosen such that the linearized system corresponding to (3) at $\mu = \mu_0$ is of the form

$$\dot{\xi} = \omega\eta,$$
$$\dot{\eta} = -\omega\xi \tag{4}$$

where $\omega = \omega(\mu_0)$ is the frequency of the linearized motion at bifurcation.

Then the stability of the bifurcating limit cycle is determined by the sign of the quantity S:

$$S = \omega(F_{\xi\xi\xi} + F_{\xi\eta\eta} + G_{\xi\xi\eta} + G_{\eta\eta\eta}) - F_{\xi\eta}(F_{\xi\xi} + F_{\eta\eta}) + G_{\xi\eta}(G_{\xi\xi} + G_{\eta\eta}) + F_{\xi\xi}G_{\xi\xi} - F_{\eta\eta}G_{\eta\eta} \tag{5}$$

where subscripts represent partial differentiation, and where all terms are to be evaluated at $\mu = \mu_0$ and at the equilibrium position $\xi = \eta = 0$.

If $S > 0$ then the limit cycle is unstable, while if $S < 0$ then it is stable. If $S = 0$ the test yields no information. ($S = 0$ represents a degenerate case in which the periodic motion may not be a limit cycle. E.g. if F and G are linear in ξ, η then $S = 0$ and a continuum of periodic motions exist for $\mu = \mu_0$.)

Application to the Stomatal Oscillator

The procedure for applying this theory to the system (2) consists of four steps:

i) Find the equilibrium point P, $x = x_0, y = y_0$.

ii) Linearize (2) around P and find the bifurcation value of $\mu = \mu_0$.

iii) Transform coordinates so that the linearized system is in the form (4).

iv) Compute S.

Let us consider these one at a time:

i) The equilibrium point P is found by requiring the RHS's of eqs. (2) to vanish. Assuming $c_2x_0 - c_3y_0 > 0$,

$$-a_1x_0 + a_2y_0 + b_1 = 0, \tag{6}$$

$$a_3x_0 - a_4y_0 + b_2 - \frac{c_1}{1 + \dfrac{1}{c_2x_0 - c_3y_0}} = 0. \tag{7}$$

Solving (6) for x_0 and substituting into (7) gives a quadratic equation for y_0. Once y_0 is known, x_0 may be found from (6). Only one set of roots (x_0, y_0) lies in the region $c_2x_0 - c_3y_0 > 0$ for values of μ near $\mu = 1$ (the value taken by Delwiche and Cooke). Thus for a given value of μ, the equilibrium point P (i.e. $x_0(\mu)$ and $y_0(\mu)$) may be found.

ii) In order to determine the stability of P, we linearize (2) around (x_0, y_0). Setting $x = u + x_0$, $y = v + y_0$ in (2), (6), (7), we obtain

$$\dot{u} = -a_1u + a_2v,$$
$$\dot{v} = [a_3 + f_x(x_0, y_0)]u + [-a_4 + f_y(x_0, y_0)]v + \cdots \tag{8}$$

where dots in the v equation represent quadratic and higher order terms, and where $f(x, y)$ is as in eqs. (2). For μ near 1 this linear system corresponds to a focus. The bifurcation value μ_0 corresponds to the transition between a stable focus and an unstable focus. The eigenvalues λ of (8) satisfy $\lambda^2 - \operatorname{tr}\lambda + \det = 0$. To find μ_0 set the trace of the matrix of the system (8) equal to zero:

$$\text{trace} = -a_1 - a_4 + \frac{c_1 c_3}{(1 + c_2 x_0 - c_3 y_0)^2} = 0. \tag{9}$$

Eqs. (6), (7), (9) may be solved for the bifurcation values of $\mu = \mu_0, x_0$ and y_0. This calculation reduces to solving a quadratic equation. We find

$$\mu_0 = 1.01026, \qquad x_0 = 11.0283, \qquad y_0 = 5.93226. \tag{10}$$

For $\mu < \mu_0$ we find P to be an unstable focus, while for $\mu > \mu_0$ P turns out to be a stable focus. Moreover we find that $d\,\mathrm{Re}(\lambda)/d\mu \neq 0$ at $\mu = \mu_0$.

At bifurcation, $\mu = \mu_0$, the equilibrium position P is a center with eigenvalues $\lambda = \pm i\omega$. Here ω^2 equals the determinant of the matrix of the system (8). We find

$$\omega = 0.856\,\alpha\,\mathrm{sec}^{-1}.$$

(See Table I for α; this motion corresponds to an oscillation with period $2\pi/\omega = 23.3$ minutes.)

This proves that a Hopf bifurcation occurs in system (2) at the values given by eqs. (10). In order to find the stability of the bifurcating limit cycle, we must put the problem into the canonical form (4) and find S.

iii) The linearized system (8) does not have the form (4) required to use the expression (5) for S. However, if we set

$$u = -a_2\xi,$$
$$v = -a_1\xi - \omega\eta$$

in (8), or equivalently,

$$x = x_0 - a_2\xi,$$
$$y = y_0 - a_1\xi - \omega\eta \tag{11}$$

in (2), we obtain

$$\dot{\xi} = \omega\eta,$$
$$\dot{\eta} = -\omega\xi + \tilde{\mathscr{G}}(\xi, \eta) \tag{12}$$

where

$$\tilde{\mathscr{G}}(\xi, \eta) = -\frac{1}{\omega}[f(-a_2\xi + x_0, -a_1\xi - \omega\eta + y_0),$$
$$-f(x_0, y_0) - f_y|_{x_0 y_0} \cdot (-a_1\xi - \omega\eta) - f_x|_{x_0 y_0} \cdot (-a_2\xi)].$$

Note that $\tilde{\mathscr{G}}(\xi, \eta)$ is a constant, $-1/\omega$, times the nonlinear terms in the Taylor expansion of $f(x, y)$ about x_0, y_0. Thus $\tilde{\mathscr{G}}(\xi, \eta)$ contains quadratic and higher order terms in ξ, η.

iv) To compute S, we identify F and G of eqs. (3) with the analogous quantities in eqs. (12):

$$F(\xi, \eta, \mu) = \omega\eta,$$
$$G(\xi, \eta, \mu) = -\omega\xi + \tilde{\mathcal{G}}(\xi, \eta). \tag{13}$$

Now the expression (5) for S contains only 2nd and 3rd derivatives of F and G with respect to ξ and η. Thus all linear terms in ξ, η do not affect S. In particular, since $\tilde{\mathcal{G}}(\xi, \eta)$ contains quadratic and higher order terms only, we may simply take $\tilde{\mathcal{G}}(\xi, \eta)$ as $-f(x, y)/\omega$ expanded about x_0, y_0 without changing S. Similarly we may drop the terms $\omega\eta$ and $-\omega\xi$ appearing in (13): We take

$$F(\xi, \eta, \mu) \equiv 0,$$
$$G(\xi, \eta, \mu) = -\frac{1}{\omega} f(-a_2\xi + x_0, -a_1\xi - \omega\eta + y_0). \tag{14}$$

Using the expression for $f(x, y)$ in eqs. (2),

$$\begin{aligned} G(\xi, \eta) &= \frac{c_1}{\omega}\left[1 + \frac{1}{c_2(-a_2\xi + x_0) - c_3(-a_1\xi - \omega\eta + y_0)}\right]^{-1} \\ &= \frac{c_1}{\omega}\left[1 + \frac{1}{(-c_2a_2 + c_3a_1)\xi + c_3\omega\eta + c_2x_0 - c_3y_0}\right]^{-1} \\ &= G(k_1\xi + k_2\eta) \end{aligned}$$

where

$$k_1 = c_3a_1 - c_2a_2 > 0 \qquad \text{from Table 1,}$$
$$k_2 = c_3\omega.$$

Table 1. Parameter values

Let $\alpha = 0.00525$. Then

$a_1 = \alpha\,\text{sec}^{-1}$,
$a_2 = \frac{13}{14}\alpha\,\text{sec}^{-1}$,
$a_3 = \frac{1}{10}\alpha\,\text{sec}^{-1}$,
$a_4 = \frac{39}{20}\alpha\,\text{sec}^{-1}$,
$b_1 = \alpha(3.57143 + 1.92857\,\mu)\,\text{bar-sec}^{-1}$,
$b_2 = \alpha(16.7857 - 0.192857\,\mu)\,\text{bar-sec}^{-1}$,
$c_1 = 19.3613\,\alpha\,\text{bar-sec}^{-1}$,
$c_2 = 0.217350\,\text{bar}^{-1}$,
$c_3 = 0.326042\,\text{bar}^{-1}$.

In equations (2), x and y are turgor pressures in bars and the independent variable is time in seconds. Delwiche and Cooke [3] model corresponds to $\mu = 1$

Here

$$G(z) = \frac{c_1}{\omega}\left[1 + \frac{1}{z + k_3}\right]^{-1}$$

where

$$k_3 = c_2 x_0 - c_3 y_0,$$
$$z = k_1 \xi + k_2 \eta.$$

We will need 2nd and 3rd derivatives of $G(z)$ for S:

$$G'(z) = \frac{c_1}{\omega}\frac{1}{(1 + z + k_3)^2},$$
$$G''(z) = \frac{c_1}{\omega}\left(\frac{-2}{(1 + z + k_3)^3}\right),$$
$$G'''(z) = \frac{c_1}{\omega}\left(\frac{6}{(1 + z + k_3)^4}\right).$$

Moreover, the chain rule gives

$$G_\xi = k_1 G'(z), \qquad G_\eta = k_2 G'(z), \qquad G_{\xi\xi} = k_1^2 G''(z), \qquad \text{etc.}$$

The expression (5) for S becomes, using eqs. (14),

$$\begin{aligned} S &= \omega(G_{\xi\xi\eta} + G_{\eta\eta\eta}) + G_{\xi\eta}(G_{\xi\xi} + G_{\eta\eta}) \\ &= k_2(k_1^2 + k_2^2)\{\omega G'''(0) + k_1 G''(0)^2\} \\ &= \frac{k_2(k_1^2 + k_2^2)c_1^2}{(1 + k_3)^6}\left\{\frac{6(1 + k_3)^2}{c_1} + \frac{4k_1}{\omega^2}\right\}. \end{aligned}$$

Since all the quantities appearing in the last expression for S are positive, S is positive and we may conclude that the limit cycle occurs only for $\mu > \mu_0$ and is unstable (as in Fig. 4(i)). This result is in agreement with numerical integrations of (2), see Fig. 3.

Other Bifurcations

As expected, the analytical results of the previous section hold only for values of the parameter μ near μ_0.

Numerical integration has revealed that as μ is increased above μ_0 the unstable limit cycle L' grows in size until it coalesces with the stable limit cycle L at $\mu_1 = 1.083^+$, see Fig. 5. For values of μ larger than μ_1 no limit cycles exist, and all motions asymptotically approach the stable equilibrium point P which lies in region II.

For values of μ just smaller than μ_0 only the stable limit cycle L exists (as the Hopf bifurcation giving rise to L' has not occurred). As μ is decreased L continues to exist until μ reaches $\mu_2 = 0.883056$. As μ decreases through μ_2 the stable limit cycle L ceases to exist (Fig. 6). This may be explained by considering the flow of system (2) in region I. As stated above, eqs. (2) are linear in region I. Eqs. (2)

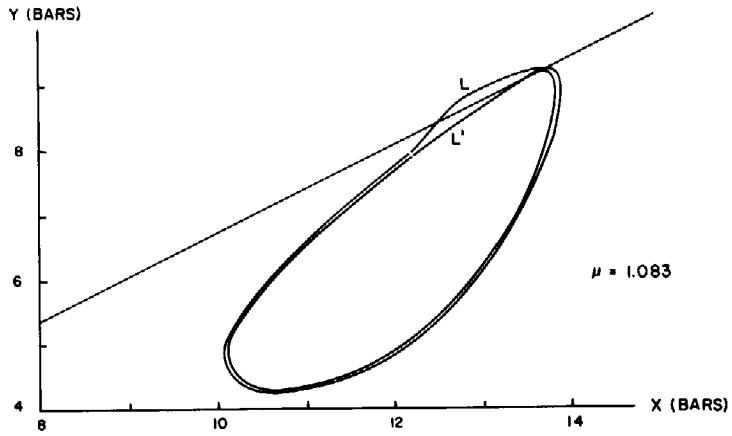

Fig. 5. Phase portrait for system (2) with $\mu = 1.083$. The stable and unstable limit cycles coalesce at $\mu = \mu_1 = 1.083^+$

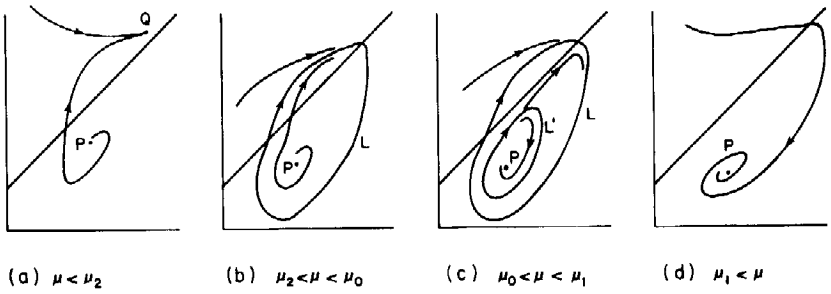

Fig. 6. Phase portraits for system (2) for various ranges of the parameter μ. ($\mu_0 = 1.01026$, $\mu_1 = 1.083^+$, $\mu_2 = 0.883056$.)

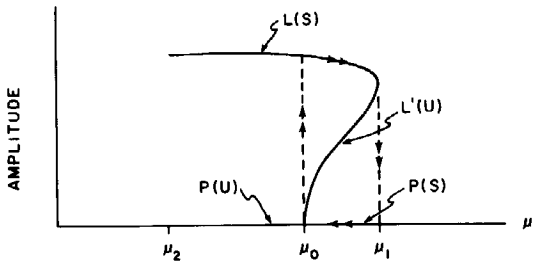

Fig. 7. Bifurcation diagram showing amplitude of periodic motions as a function of parameter μ. Double arrows show hysteresis loop and jump phenomena which occur if μ is considered to vary quasistatically. *U, unstable*; *S, stable*

with $f(x, y) \equiv 0$ possess an equilibrium point Q which is a stable node for all values of μ, but which lies in region I only if $\mu < \mu_2$. Thus as μ is decreased through μ_2 a stable equilibrium point Q appears on the line $c_2x = c_3y$ at $\mu = \mu_2$ and Q moves into region I for $\mu < \mu_2$, causing the sudden elimination of the stable limit cycle L. For values of μ smaller than μ_2 all motions asymptotically approach the stable equilibrium point Q.

The qualitative dynamics of system (2) for μ near unity are summarized in Figs. 6 and 7.

Discussion

As mentioned in the introduction, an increase in the parameter μ represents an increase in the quantity of osmotica in the guard cell. For μ sufficiently large it is to be expected that the stomatal pore will remain open, as follows: An increase in guard cell osmotica will cause water to diffuse into the guard cell from the neighboring subsidiary cells; this will increase guard cell turgor x and decrease subsidiary cell turgor y whereupon the pore width w will increase in accordance with eq. (1).

Similarly it is to be expected that the stomatal pore will remain closed if μ is sufficiently small.

These two situations are represented by Figs. 6d and 6a, respectively. For $\mu > \mu_1$ all motions asymptotically approach point P in region II ($w > 0$) while for $\mu < \mu_2$ point P is unstable and all motions asymptotically approach point Q in region I ($w \equiv 0$).

For $\mu_2 < \mu < \mu_0$ all motions asymptotically approach the stable limit cycle L, Fig. 6b, which lies partly in region I ($w \equiv 0$) and partly in region II ($w > 0$). This case includes $\mu = 1$, the case originally chosen by Delwiche and Cooke [3].

For $\mu_0 < \mu < \mu_1$ we have two limit cycles L, L', as in Fig. 6c. All motions which have initial conditions inside the unstable limit cycle L' will asymptotically approach the stable equilibrium P, while all other motions approach the stable limit cycle L. This represents a *threshold* phenomena: in order for the oscillation L to be excited, the system must start out sufficiently far from point P.

Now consider Fig. 7 which shows the amplitude of the periodic motions as a function of μ. If we consider μ to vary in a quasistatic fashion with time, Fig. 7 reveals that the system (2) exhibits *hysteresis* and jump phenomena. Consider, for example, a point moving along the upper portion of the curve in Fig. 7 as μ is increased. When μ becomes larger than μ_1 the stable limit cycle L disappears and such a point "jumps" down to the stable equilibrium P. If μ is now decreased such a point remains at P even though L has reappeared (due to the threshold phenomenon described previously). When μ becomes smaller than μ_0, however, P changes from stable to unstable and the system jumps up to L once again.

If μ is decreased from a value above μ_1 to a value below μ_2 the system evolves from a steady state open pore P to a steady state closed pore Q, with an intermediary state of stable oscillation L. From this point of view the limit cycles L and L' provide the system with a kind of dynamical "bridge" between the equilibrium states P and Q.

In conclusion, this work shows that the model proposed by Delwiche and Cooke [3] can exhibit a diversity of dynamic behavior, including a Hopf bifurcation and other bifurcations. The model is very sensitive to parameter variations, at least in the range of parameters originally chosen in [3].

References

1. Cooke, J. R., DeBaerdemaeker, J. G., Rand, R. H., Mang, H. A.: A finite element shell analysis of guard cell deformations. Trans. ASAE **19**, 1107–1121 (1976)

2. Barrs, H. D.: Cyclic variations in stomatal aperture, transpiration, and leaf water potential under constant environmental conditions. Ann. Rev. Plant Physiol. **22**, 223–236 (1971)
3. Delwiche, M. J., Cooke, J. R.: An analytical model of the hydraulic aspects of stomatal dynamics, J. Theor. Biol. **69**, 113–141 (1977)
4. Marsden, J. E., McCracken, M.: The Hopf bifurcation and its applications, pp. 408. Berlin-Heidelberg-New York: Springer-Verlag 1976

Received August 19/Revised December 15, 1980